INTERNATIONAL SOCIETY FOR SOIL MECHANICS AND GEOTECHNICAL ENGINEERING



This paper was downloaded from the Online Library of the International Society for Soil Mechanics and Geotechnical Engineering (ISSMGE). The library is available here:

https://www.issmge.org/publications/online-library

This is an open-access database that archives thousands of papers published under the Auspices of the ISSMGE and maintained by the Innovation and Development Committee of ISSMGE.



STRAIN COMPATIBILITY SIMULATION OF REINFORCED SOIL STRUCTURES ANALYSE EN DEFORMATION DU COMPORTEMENT DES OUVRAGES EN SOLS RENFORCES

Ilan Juran¹ Khalid Farrag²

¹Chairman, Civil Engineering Department, Polytechnic University, Brooklyn, New York, U.S.A.

²Research Coordinator, Geosynthetics Engineering Lab

Louisiana Transportation Research Center, Baton Rouge, Los Angeles, U.S.A.

ABSTRACT

The strain compatibility method, developed by Juran et al. (1990), is assessed through the analysis of the behavior of several instrumented and well-documented reinforced soil walls and embankments. The instrumented structures were constructed as a part of a Federal Highway Administration (FHWA) project (Christopher et al., 1989), and their behavior has been analyzed using the Finite Element method by Adib (1988) and Adib et al. (1990). The strain compatibility analysis permits an evaluation of the effect of the reinforcement extensibility and soil properties on the state of stress in the reinforced-soil structures. The analytical predictions are compared with the measured field behavior, and the effects of the soil and reinforcement parameters on the state of stress in the reinforced-soil structures are evaluated.

MODELING REINFORCED SOIL STRUCTURES

The strain compatibility approach, proposed by Juran et al. (1990), for the analysis of geosynthetics-reinforced soil walls has been assessed through numerical simulations of the reinforced soil response in direct shear (Juran et al., 1988), and was discussed in detail in preceding papers (Juran et al., 1990 and Farrag and Juran, 1992). A brief outline of the main design assumptions is presented herein.

The soil is assumed to be an elasto-plastic strain hardening material with a non-associated flow rule. The yield criteria can be written as:

$$F(\sigma_{ij}, \gamma_{xy}) = \frac{\tau_{xy}}{\sigma_{y}} - h(\gamma_{xy}) = 0$$
 (1)

where γ_{xy} is the shear strain, σ_y and τ_{xy} are the mobilized normal and shear stresses along the potential failure surface, and $h(\gamma_{xy})$ is the strain hardening function.

The non-associated plastic flow of the soil during simple shearing is assumed to follow the stress ratio-dilatancy relationship (with the elastic strain assumed negligible):

$$tanu = \frac{de_y}{d\gamma_{xy}} = \frac{1}{\mu_x} \left[tan\phi_{cv} - \frac{\tau_{xy}}{\sigma_y} \right]$$
 (2)

where ν is the dilatancy angle, $d\varepsilon_{y}$ is soil strain normal to the failure surface, $d\gamma_{xy}$ is shear strain, ϕ_{cv} is the critical state friction angle of the soil and μ_{1} is a factor which equals μ_{1} for contracting behavior and μ_{2} for dilating behavior.

The reinforcement is assumed to be an elastic perfectly plastic material. The shear strain distribution $d\gamma_{sy}$ along the assumed potential failure surface is assumed to be linearly increasing with depth. A schematic diagram of a soil layer along the potential failure surface is depicted in Figure 1.

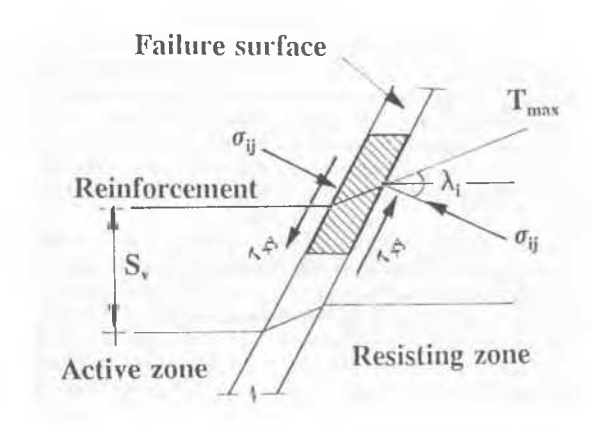


Figure 1. A schematic diagram of the state of stresses along the failure surface

For the soil layer along the failure surface, the soil strain in the direction of the reinforcement $d\epsilon_a$ is given by:

$$de_{p} = \tan v_{m} \left[1 - \frac{\cos \left(\lambda_{i} - v_{m}\right) \cdot \sin \lambda_{i}}{\sin v_{m}}\right] d\gamma_{xy}$$
 (3)

where v_m is the mobilized soil dilatancy angle and λ_i is the inclination of the reinforcement with respect to the failure surface at reinforcement layer i.

The assumption of strain compatibility between the soil and the reinforcement (i.e. $d\epsilon_p = d\epsilon_R$, where $d\epsilon_R$ is the strain in the reinforcement) permits the calculation of the tension force increment $d\sigma_R$ in the reinforcement, i.e.

$$d\sigma_R = E \cdot d\varepsilon_R$$
 (4)

where E is the reinforcement elastic modulus.

For an assumed failure surface, the analysis of the horizontal and vertical equilibrium of the active zone stability wedge yields a non-dimensional solution relating the maximum tension forces at each reinforcement layer T_N and the non-dimensional structure height H/h_e , where H is the actual wall height and h_e is the relative stiffness of the reinforced soil mass. h_e is defined

$$h_o = E. t. b/\rho . H. S_h. S_v$$
 (5)

where t and b are the thickness and width of the reinforcement, respectively; ρ is the soil unit weight; and S_h and S_v are the horizontal and vertical spacings between the reinforcement, respectively. The maximum tension force T_N is given by the non-dimensional parameter:

$$T_{N} = T_{\text{max}} / \rho \cdot H \cdot S_{h} \cdot S_{v} \tag{6}$$

The incremental analysis was implemented in a computer program (Juran et al. 1988) which yields for each shear strain increment the location of the critical potential failure surface; i.e., the failure surface corresponding to the minimum height under the specified shear strain increment.

The relationship between T_N and H/h_o is illustrated in Figure 2 for a typical compacted backfill material with a soil friction angle at peak $\phi_p = 40^\circ$, soil friction angle at critical state $\phi_{cv} = 31^\circ$, soil unit weight $\rho = 15.5 \text{ KN/m}^3$, constant soil dilatancy angle $\nu = 1/3 \phi$, and a range of normalized shear moduli (G/σ_v) .

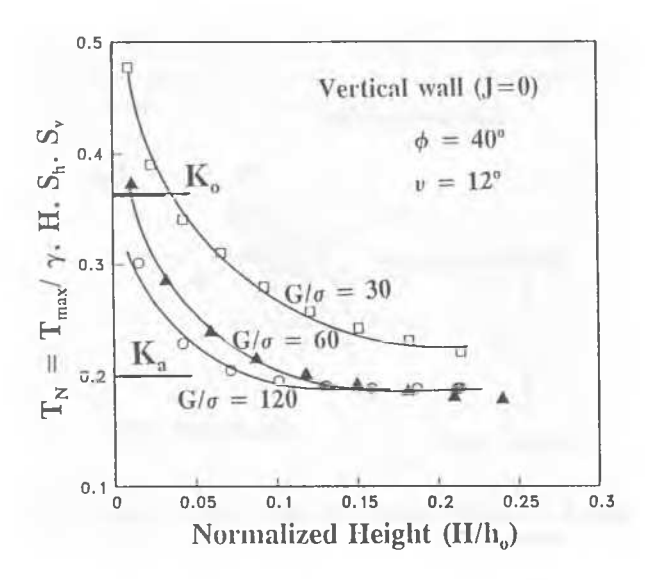


Figure 2. Effect of relative stiffness h, on the tension forces

Figure 2 illustrates the effect of the relative stiffness h_o on the state of stresses in the soil. For a high value of h_o (e.g. for quasi-inextensible reinforcement) the normalized tension forces are close to those calculated for a K_o state of stress. As h_o decreases (e.g. for more extensible reinforcement or higher S_v and S_h values), the tension forces approach those calculated for a K_o state of stress. The state of stress in the soil is also affected by the soil shear modulus G and the confining pressure σ_y . An increase in the normalized soil modulus G/σ leads to a decrease in the normalized tension forces for the same H/h_o values.

ANALYSIS OF REINFORCED SOIL WALLS

The strain compatibility approach is implemented in the analysis of the state of stress in the soil and tension forces in the reinforcement of the FHWA reinforced soil test walls documented by Christopher et al. (1989) and simulated using FE analysis by Adib et al. (1990). Five reinforced soil walls, constructed with different soil-and reinforcement types, are analyzed. The walls are 6 m (20 ft) high. The soil and reinforcement parameters used in the analysis are obtained from the above-cited references and are presented in Table 1. It should be noted that soil parameters are dependent on the applied confining stress. Therefore, average soil parameters are chosen to represent its behavior within a given range of confining pressures.

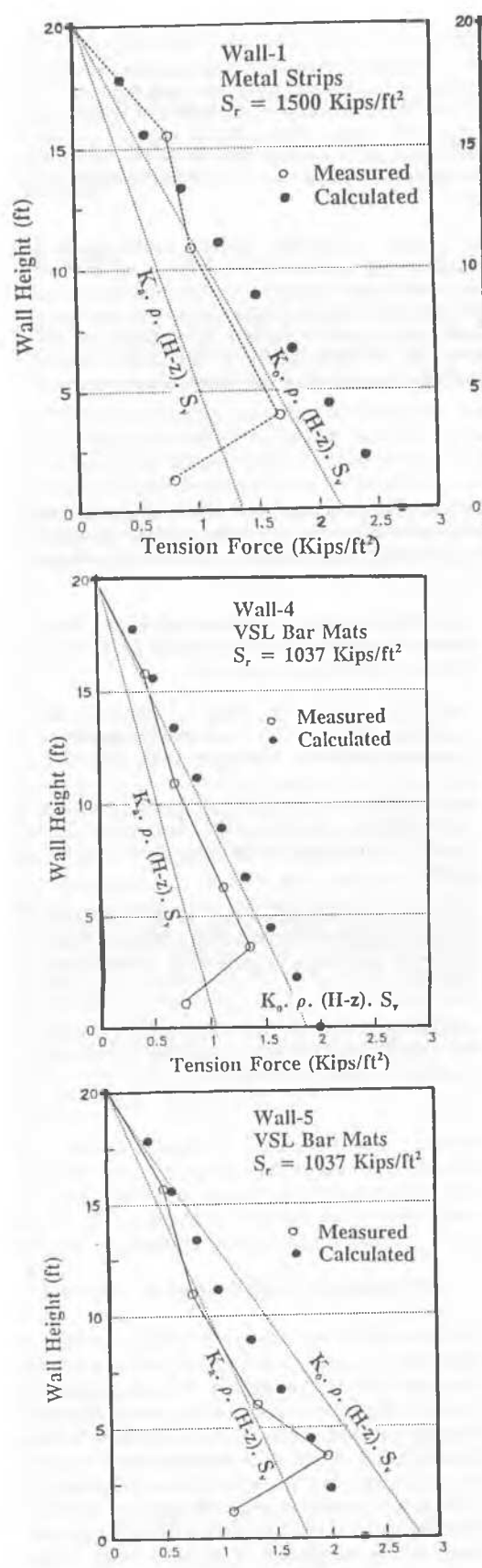
Table 1. Reinforced-wall parameters used in the wall analysis

Wall	1	2	3	4	5
-Height (ft) -Soil type	20 sand-	20 sand-	20 sand-	20 cobble	20 silt
-Soil unit wt.	gravel 0.13	gravel 0.13	gravel 0.13	0.105	0.13
-Friction angle -Cohesion C	40 0	40 0	40 0	42 0	35 0.05
(Kips/ft²) -Soil elasticity modulus*, E	220	220	220	300	100
(Kips/ft²) -Soil shear	60	60	60	100	35
modulus / normal stress (G/σ°) -Reinforcement	steel	geogrid	bar	bar	bar
type -S.** (Kips/ft²)	strips 1500	geogriu 56	mats 1037	mats 1037	mats 1037
-S _b (ft) -S _v (ft)	2.4 2.5	contin. 2.5	4.95 2.5	4.95 2.5	4.95 2.5
-H/h。	0.0016	0.0465	0.0025	0.002	0.0025

- 1 ft = 0.305 m, 1 Kips/ft² = 48.82 KN/m², 1 Kips/ft³ = 157.2 KN/m³
- * Calculated from the hyperbolic model parameters (Adib, 1988)
- ** S_r is reinforcement stiffness and equals to E.t.b/ $S_h.S_v$. It is related to the relative reinforcement stiffness h_o in this analysis by: $h_o = S_r/\rho$
 - S_h is the horizontal spacing between the reinforcement
 - S, is the vertical spacing between the reinforcement.

Figures 3-a to 3-e show the calculated and measured maximum tension forces along the reinforcement in walls 1 to 5, respectively. The measured maximum tension forces were evaluated from measurements along the reinforcement (Christopher, 1989). The calculated tension forces in the reinforcement were evaluated along the critical potential failure plane. The measured tension forces compares fairly well with the measured tension forces in the walls. The differences observed between predicted and measured tension forces at the bottom of the five walls may be partially due to the boundary effects of the foundation soil which probably restrain the lateral displacement and thereby decrease the lateral stresses at the lower parts of the walls.

The measured and predicted tension forces seem to range between the cases of K_o and K_a states of stress for the range of soil and reinforcement properties utilized for these walls. Both the calculated and measured forces are close to the K_o state of stress at the upper part of the walls and approach the K_a state of stress at the lower part. At the upper part of the walls, the soil dilatancy seems to increase the normal stresses applied to the reinforcement, thus increasing the mobilized tension forces. The effect of soil dilatancy is minimum under higher confining pressures at the lower parts of the walls.



Tension Force (Kips/ft2)

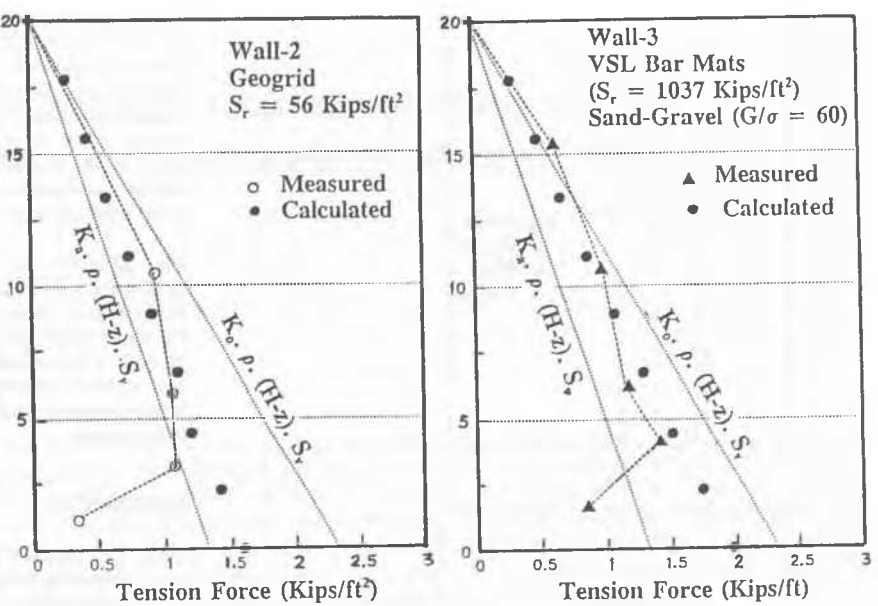


Figure 3. Calculated and measured tension forces in the walls

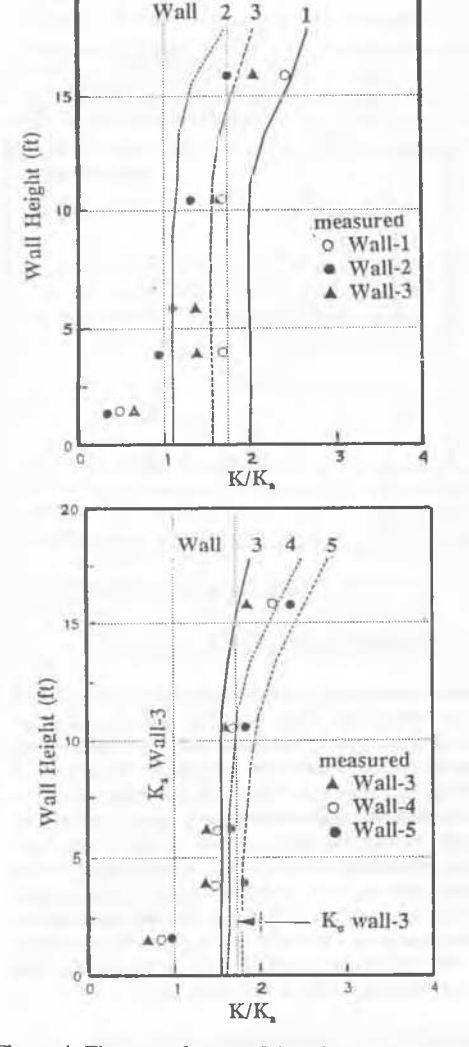
The effect of reinforcement extensibility is demonstrated through the analysis of walls 1,2 and 3. The three walls with the same soil properties are constructed using three different types of reinforcement. The measured and predicted tension forces in the three walls are normalized with respect to Rankine's state of stress K_n in Figure 4-a. The mobilized tension forces in wall 1, with the quasi-inextensible reinforcement (H/ h_o equals 0.0016), are close to K_o state of stress, whereas the tension forces in wall 2, with more extensible reinforcement, are mobilized close to a K_o state of stress. As the reinforcement extensibility increases, the mobilized tension forces decrease from the K_o state to the K_o state of stress. The figure also demonstrates the effect of the overburden pressure on the development of the state of stress along the wall height. The distribution of tension forces is close to K_o at the upper part of the walls and approaches K_o at the lower part.

The effect of soil properties on the mobilized tension forces in the reinforcement is illustrated through the comparison of walls 3,4 and 5. The three walls are constructed using the same type of reinforcement, VSL bar mats. Soil types differ from a relatively high G/σ of 100 in wall 4 to G/σ of 35 in wall 5. In these walls, the measured and calculated tension forces are normalized with their respective values of K_a in Figure 4-b. For walls 3 and 5, with equal values of H/h_o , the figure shows that, as G/σ decreases, the tension forces increase and approach the K_a state of stress.

ANALYSIS OF REINFORCED SLOPES

The numerical procedure was utilized to simulate the state of stress of a reinforced soil embankment documented by Christopher et al. (1989). The embankment slope was 0.5 horizontal to 1 vertical with a height of 6.5 m (20 ft). The embankment was constructed using silty soil with soil parameters identical to those of wall-5. Eight layers of woven-geotextile reinforcement with a uniform spacing (S_v) of 0.76 m (2.5 ft) and total length of 4.27 m (14 ft) were used. Since the cohesion effect is not yet implemented in the analytical procedure, the analysis was carried out assuming c=0.

Figure 5 shows the comparison between the measured and calculated maximum tension forces in the reinforcement. The calculations of the tension forces are carried out considering both a variable and a fully mobilized constant dilatancy angle of $\nu=1/3~\phi$. The calculated tension forces compare fairly well with the measured values in the reinforced slope. The assumption of a constant dilatancy angle seems to give an upper bound of the developed tension forces.



20

Figure 4. The state of stress of the reinforcement with depth

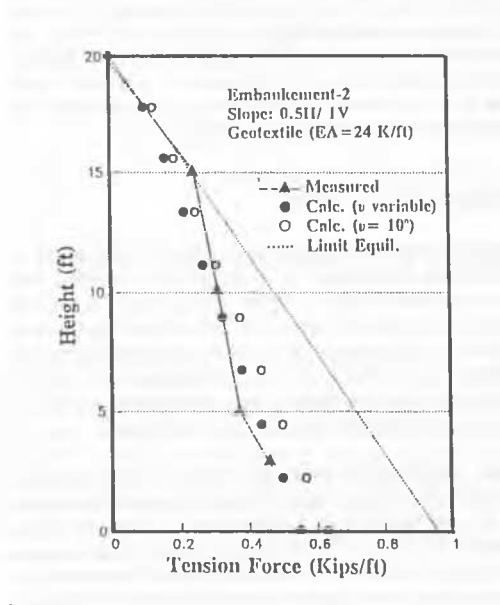


Figure 5. Calculated and measured tension forces in the embankment

CONCLUSIONS

The strain compatibility analysis was evaluated through comparisons with the measured tension forces in instrumented walls and embankments. The comparisons demonstrate the applicability of the method to predict the tension forces in the reinforcement. The analytical approach and the observations of the instrumented structures demonstrate the effect of reinforcement extensibility and soil properties on the mobilized tension forces in the reinforcement.

The application of a strain compatibility analysis requires properly established soil parameters and mechanical properties of the confined reinforcement. These parameters are dependent upon the confining pressures and can be significantly affected by soil compaction and construction process. There is a substantial need to establish reliable testing procedures and interpretation methods for the determination of the in-situ confined reinforcement properties for an appropriate design of geosynthetics reinforced soil structures.

REFERENCES

- Adib., M., Mitchell, J.K., and Christopher, B.R., (1990), "Finite Element Modeling of Reinforced Soil Walls & Embankments," Design & Performance of Earth Retaining Structures, ASCE, GSP No. 25, pp. 409-424.
- Adib,, M., (1988), "Lateral Earth Pressure in Reinforced Soil Walls," Thesis Submitted in Partial Satisfaction of the Requirements for the Ph.D. Degree, University of California, Berkeley, CA.
- Christopher, B.R., Gill, S.A., Giroud, J.P., Juran, I., Mitchell, J.K., Schlosser, F., and Dunnicliff, J., (1989), "Reinforced Soil Structures, Design and Construction Guidelines," FHWA Report No. RD-89-043.
- Farrag, K., and Juran, I., (1992), "Design of Geosynthetic Reinforced Soil Structures," Proceedings, Grouting, Soil Improvement and Geosynthetics, ASCE, Geotechnical Special Publication No. 30, Vol. 2, pp. 1188-1200.
- Juran, I., Ider, H., Chen, C., and Guermazi, A., (1988), "Numerical Analysis of Response of Reinforced Soils to Direct Shearing," Inter. Journal of Numerical and Analytical Methods in Geomechanics, Vol.12, pp. 157-171.
- Juran, I., Ider, H., and Farrag, K., (1990), "Strain Compatibility Analysis for Geosynthetic Reinforced Soil Walls," *Journal of Geotechnical Engineering*, ASCE, Vol. 116, pp. 312-329.